

# A system of three transiting super-Earths in a cool dwarf star

E. Díez Alonso,<sup>1</sup> S. L. Suárez Gómez,<sup>1</sup> J. I. González Hernández,<sup>2,3</sup>  
 A. Suárez Mascareño,<sup>4</sup> C. González Gutiérrez<sup>1</sup>, S. Velasco<sup>2,3</sup>, B. Toledo–Padrón<sup>2,3</sup>,  
 F. J. de Cos Juez<sup>1★</sup>, R. Rebolo<sup>2,3,5</sup>

<sup>1</sup>*Department of Exploitation and Exploration of Mines, University of Oviedo, Oviedo, Spain*

<sup>2</sup>*Instituto de Astrofísica de Canarias, E-38205 La Laguna, Tenerife, Spain*

<sup>3</sup>*Universidad de La Laguna, Dpto. Astrofísica, E-38206 La Laguna, Tenerife, Spain*

<sup>4</sup>*Observatoire Astronomique de l'Université de Genève, 1290 Versoix, Switzerland*

<sup>5</sup>*Consejo Superior de Investigaciones Científicas, Spain*

Accepted XXX. Received YYY; in original form ZZZ

## ABSTRACT

We present the detection of three super-Earths transiting the cool star LP415-17, monitored by K2 mission in its 13<sup>th</sup> campaign. High resolution spectra obtained with HARPS-N/TNG showed that the star is a mid-late K dwarf. Using spectral synthesis models we infer its effective temperature, surface gravity and metallicity and subsequently determined from evolutionary models a stellar radius of  $0.58 R_{\odot}$ . The planets have radii of 1.8, 2.6 and  $1.9 R_{\oplus}$  and orbital periods of 6.34, 13.85 and 40.72 days. High resolution images discard any significant contamination by an intervening star in the line of sight. The orbit of the furthest planet has radius of 0.18 AU, close to the inner edge of the habitable zone. The system is suitable to improve our understanding of formation and dynamical evolution of super-Earth systems in the rocky – gaseous threshold, their atmospheres, internal structure, composition and interactions with host stars.

**Key words:** planets and satellites: detection – techniques: photometric – techniques: spectroscopic – stars: low mass – stars: individual: LP415-17

## 1 INTRODUCTION

Transiting planetary systems are of great value for the characterization of exoplanetary atmospheres (Charbonneau et al. 2000; Kreidberg et al. 2014), the understanding of planetary formation and evolution (Owen et al. 1999) and for the study of the interactions with their host stars (Cauley et al. 2017). Cool dwarf stars are well suited to find Earth size and super-Earth size planets by the transit method, since transits produce deeper dimmings than in solar-type stars. The amplitude of signals in transit transmission spectroscopy is also higher for stars with small radius, favoring these type of stars for future atmospheric studies of their planetary systems (Gillon et al. 2016).

The Kepler mission (Borucki et al. 2010) has achieved a large number of detections of transiting planets

(Howard et al. 2012). In its second mission (Howell et al. 2014), the satellite performs observations of different ecliptic plane fields for periods of time spanning about 80 days. Multiple signals of exoplanet candidates are present in concluded campaigns (Vanderburg et al. 2015; Crossfield et al. 2016). Campaign 13<sup>th</sup> has focused in the Hyades and Taurus region, centered in  $\alpha=04:51:11$ ,  $\delta=+20:47:11$ , between 2017 March 08<sup>th</sup> and 2017 May 27<sup>th</sup>. In this campaign K2 observed 26.242 targets at standard long cadence mode and 118 targets at short cadence mode. LP415-17 ( $\alpha=04:21:52.487$ ,  $\delta=+21:21:12.96$ ) has been observed in low cadence mode.

In this letter, we present the detection of three super-Earths transiting the star LP415-17 (EPIC 210897587, 2MASS 04215245+2121131). In section 2 we describe the characterization of the star from spectra acquired with HARPS-N spectrograph and the analysis of the K2 photometric time series. We also discuss possible contaminating sources and the main parameters derived for the planets. In section 3 we present estimations of the masses, discuss the

★ E-mail: fjc@uniovi.es

stability of the system and its suitability for future characterization by transmission spectroscopy. In section 4 we summarize the main conclusions derived from this work.

## 2 METHODS

### 2.1 Stellar characterization

We obtained three spectra, 1800 seconds of exposure time each, with HARPS-N (Cosentino et al. 2012) a fibre-fed high resolution echelle spectrograph installed at the 3.6 m Telescopio Nazionale Galileo in the Roque de los Muchachos Observatory (Spain) with a resolving power of  $R = 115,000$  over a spectral range from 380 to 690 nm. We have averaged them to obtain a final spectrum smoothed with 10-pixel step to improve the visualization of spectral features. We compared this spectrum with synthetic models (Allende Prieto et al. 2014) generated with ASSET (Koesterke et al. 2008), adopting Kurucz atmospheric models (Castelli & Kurucz 2003; Mészáros et al. 2012). Synthetic spectra have been broadened with a macroturbulence profile of 1.64 km/s (Fischer & Valenti 2005), with a rotation profile taking  $v_{rot} = 1.6$  km/s Gray (2005) and with a gaussian profile for instrumental broadening at resolution of 115,000 (FWHM  $\sim 2.6$  km/s). The effective temperature has been estimated using the infrared flux method (González Hernández & Bonifacio 2009). We apply  $T_{IRFM} - (\text{color}, [\text{Fe}/\text{H}])$  calibrations for dwarf stars, correcting for extinction the stellar magnitudes according to  $A_X = R_X \times E(B - V)$ .  $R_X$  was obtained from McCall (2004), and the reddening  $E(B - V)$  from the dust maps (Schlegel et al. 1998), but corrected using the equations in Bonifacio et al. (2000) for the estimated distance to the star (82 pc) and galactic latitude. We obtained  $E(B - V) = 0.087$  and  $T_{IRFM} = 4258 \pm 150$  K.

The metallicity and  $\log g$  have been obtained via comparison of the observed spectrum with synthetic spectra, resulting  $[\text{Fe}/\text{H}] = -0.3 \pm 0.2$  and  $\log g = 4.6 \pm 0.3$  (Fig. 1). We compare the stellar parameters and metallicity with a grid of tabulated isochrones (Bertelli et al. 1994), and obtain  $R_* = 0.58^{+0.06}_{-0.03} R_\odot$ ,  $M_* = 0.65^{+0.06}_{-0.03} M_\odot$  and  $M_V = 7.95^{+0.34}_{-0.66}$  mag. In Fig. 2 we compare the observed spectrum of LP415-17 with that of the well characterized star HD199981 (Kordopatis et al. 2013), whose parameters ( $K6V$ ,  $T_{\text{eff}} = 4263\text{K}$ ,  $\log g = 4.97$ ) are very close to our results for LP415-17.

Adopting  $m_V = 12.54$ , we estimate a distance to LP415-17 of  $D_* = 82^{+29}_{-12}$  pc. We measured a radial velocity from the HARPS-N spectrum, which combined with the proper motions reported in Table 1 results in velocity components  $U = -38.2$  km/s,  $V = -69.4$  km/s,  $W = 31.8$  km/s. A comparison with the kinematic and metallicity properties of the Copenhagen Survey of the Solar neighbourhood (Nordström et al. 2004), suggests that LP 415-17 could be a member of the Hercules stream, which according to Bensby et al. (2007) could be a combination of thin and thick disk stars originating in interactions of the inner disk with the bar of our Galaxy.

We analyzed photometry from SuperWASP (Pollacco et al. 2006). 5819 data points, after 2.5  $\sigma$  clip to remove outliers (Suárez Mascareño et al. 2016),

**Table 1.** Stellar parameters for LP415-17.

Parameter	Value	Source
V [mag]	$12.806 \pm 0.005$	(1)
R [mag]	$12.286 \pm 0.006$	(1)
I [mag]	$12.289 \pm 0.090$	(1)
J [mag]	$10.274 \pm 0.021$	(2)
H [mag]	$9.686 \pm 0.021$	(2)
K [mag]	$9.496 \pm 0.014$	(2)
$T_{\text{eff}}$ [K]	$4258 \pm 150$	(3)
$[\text{Fe}/\text{H}]$	$-0.3 \pm 0.2$	(3)
Radius [ $R_\odot$ ]	$0.58^{+0.06}_{-0.03}$	(3)
Mass [ $M_\odot$ ]	$0.65^{+0.06}_{-0.03}$	(3)
$\log g$ [cgs]	$4.6 \pm 0.3$	(3)
$M_V$ [mag]	$7.95^{+0.34}_{-0.66}$	(3)
$\log_{10}(R'_{HK})$	$-4.85 \pm 0.13$	(3)
$P_{rot}$ [d]	$29.6 \pm 0.4$	(3)
Distance [pc]	$82^{+29}_{-12}$	(3)
$V_r$ [km/s]	$19.1 \pm 0.5$	(3)
$\mu_\alpha$ [mas/y]	$201.9 \pm 6.9$	(1)
$\mu_\delta$ [mas/y]	$-71.3 \pm 4.3$	(1)
U, V, W [km/s]	$-38.2, -69.4, 31.8$	(3)

(1) UCAC4 (Zacharias et al. 2013).

(2) 2MASS (Cutri et al. 2003).

(3) This work.

spanning 1325 days. A Lomb – Scargle periodogram (Scargle 1982) was performed, obtaining the strongest signal at  $0.0338 \pm 0.005 d^{-1}$  ( $29.6 \pm 0.4$  days), that we relate to stellar rotation. From the observed spectrum we determine a  $R'_{HK}$  index of  $-4.85 \pm 0.13$  which according to Suárez Mascareño et al. (2015, 2016) indicates a likely rotation period of  $34.8 \pm 8.2$  days. Table 1 summarizes stellar parameters for LP415-17.

### 2.2 K2 photometric data

The light curve of LP415-17 exhibits clear signals of at least three transiting objects (Fig. 3). We analyzed the K2 corrected photometry from the star following the work of Vanderburg & Johnson (2014), applying a spline fit to detrend stellar variability and search for periodic signals with a Box Least Squares (BLS) method (Kovács et al. 2002) on flattened data. Once BLS finds a transit signal, it is fitted, removed and another search for transit signals is performed. Following this method, we find three transit signals of planet candidates with orbital periods  $6.342 \pm 0.002$  days (b),  $13.850 \pm 0.006$  days (c) and  $40.718 \pm 0.005$  days (d).

Planet d only shows two transits in the K2 13<sup>th</sup> campaign observation window. Separate analysis of these two transits performing Markov Chain Monte Carlo (MCMC) (Eastman et al. 2013) reveals coincident transit parameters, supporting the idea that this signal is created by the same object. The parameters for each observed transit of planet d are summarized in Table 2.

We analyzed each phase-folded transit using MCMC to estimate the main parameters for each planet (Fig. 4). We assumed priors on host star ( $T_{\text{eff}} = 4258\text{K}$ ,  $\log g = 4.6$ ,  $[\text{Fe}/\text{H}] = -0.3$ ), orbital periods ( $P_{orb} = 6.34$  (b), 13.85 (c), 40.72 (d) days and assumed eccentricity  $e = 0$  due to tidal circularization of the orbits (Van Eylen & Albrecht 2015). The parameters obtained for planets b, c and d are summarized in Table 2.

The planets have estimated radii  $1.8^{+0.2}_{-0.1} R_\oplus$  (b),  $2.6^{+0.7}_{-0.2} R_\oplus$  (c) and  $1.9^{+0.7}_{-0.2} R_\oplus$  (d), orbital periods  $6.342 \pm 0.002$  days

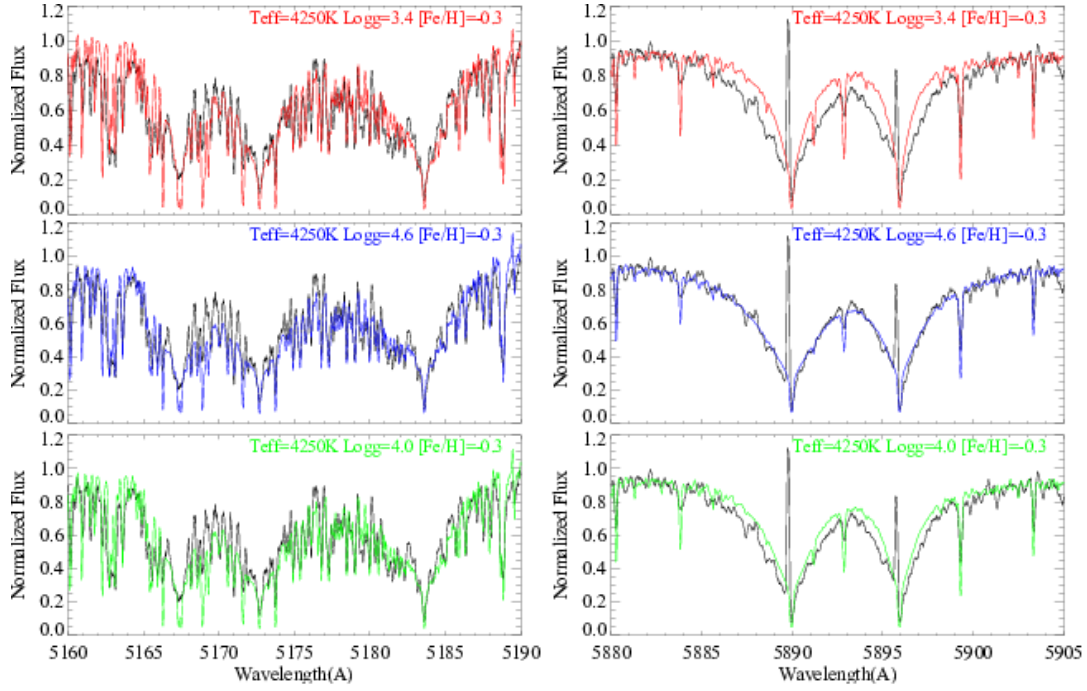


**Figure 1.** Synthetic spectral models centered in the magnesium triplet (left) and Na D doublet (right), calculated with  $T_{\text{eff}}=4250$  K,  $[\text{Fe}/\text{H}]=-0.3$  and  $\log g = 3.4$  (top),  $\log g = 4.6$  (middle) and  $\log g = 4.0$  (bottom), compared with the observed spectrum. The best fit is obtained with  $\log g = 4.6$ . No attempt has been made to reproduce with spectral synthesis the emission detected in the core of the Na D lines.

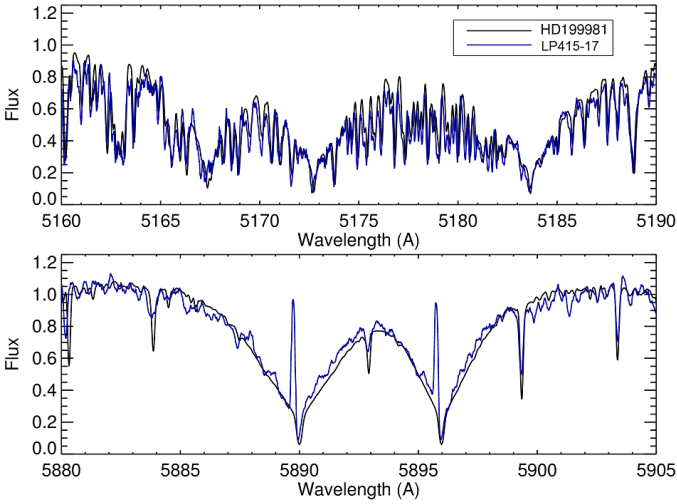


**Figure 2.** Smoothed spectrum of LP415-17 compared with the observed spectrum of HD 199981.

(b),  $13.850 \pm 0.006$  days (c) and  $40.718 \pm 0.005$  days (d), and semimajor axis  $0.0562^{+0.0013}_{-0.0014}$  AU (b),  $0.0946^{+0.0031}_{-0.0030}$  AU (c) and  $0.1937^{+0.0064}_{-0.0059}$  AU (d).

### 2.3 False positives analysis

To exclude false positives from possible companions, we analyzed speckle images of the star at 562 and 832 nm, obtained with NESSI at the 3.5 meters WIYN telescope

(Kitt peak, Arizona), available at ExoFOP-K2<sup>1</sup>. Images exclude companions at 0.2 arcseconds with  $\delta\text{mag} < 3.5$  and at 1 arcsecond with  $\delta\text{mag} < 6$ . We searched for possible contaminating background sources in images from POSS-I (Minkowski & Abell 1963) (year 1953) and 2MASS (Cutri et al. 2003) (year 1998). LP415-17 exhibits high proper motion  $\mu_\alpha = 201.9$  mas/year  $\mu_\delta = -71.3$  mas/year so we can inspect for background sources at LP415-17's position during the K2 13<sup>th</sup> campaign. No background object is found at the current star position (Fig. 5).

Speckle images from WIYN, inspection of POSS-I and 2MASS images and estimates of false positive probability for systems with three candidates at  $< 0.4\%$  (Lissauer et al. 2011) make us to reject possible contaminating sources, concluding that the transit signals in LP 415-17 are of planetary origin.

## 3 DISCUSSION

Following the mass – radius relation (Weiss & Marcy 2014)

$$\frac{M_p}{M_\oplus} = 2.69 \cdot \left( \frac{R_p}{R_\oplus} \right)^{0.93}$$

for planets satisfying  $1.5 \leq R_p/R_\oplus \leq 4$ , we obtain  $M_b = 4.7 M_\oplus$ ,  $M_c = 6.5 M_\oplus$ ,  $M_d = 4.9 M_\oplus$  for planets b, c, and d, respectively. Assuming  $M_p \ll M_*$ , circular orbits and  $\sin i \sim 1$ , we compute induced amplitudes in stellar velocity variations of 2.2 m/s for planet b, 2.3 m/s for planet c and 1.2 m/s for planet d.

<sup>1</sup> <https://exofop.ipac.caltech.edu/k2/>

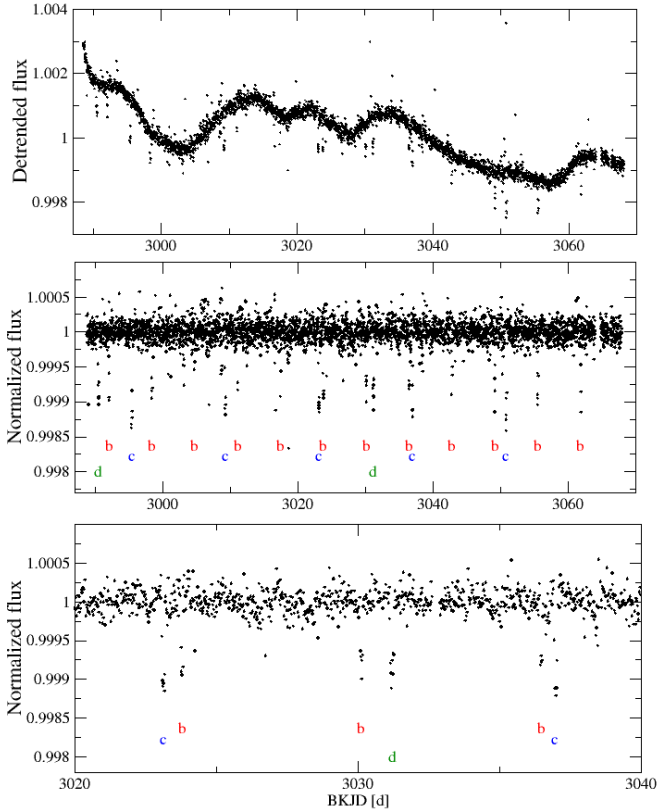


**Figure 3.** Top: K2 detrended light curve for LP415-17. Middle: normalized light curve. Characters b, c and d indicate times of observed transits of planets b, c and d. Bottom: normalized light curve zoomed between BKJD = 3020 and BKJD = 3040.

Given the visual magnitude of the star ( $V=12.8$ ) the required radial velocity monitoring at 1 m/s precision is hard to obtain for HARPS-like spectrographs in medium size telescopes, however is well suited for ESPRESSO (Pepe et al. 2014; González Hernández et al. 2017) at the VLT. The moderated chromospheric activity of the star is likely to induce RV signals of order less than 3 m/s (Suárez Mascareño et al. 2017) which should not prevent the detection of the dynamical signals induced by the planets and the determination of their masses and densities. We estimate the incident flux for planet d as  $F_p=2.63 F_\oplus$ . Habitable zone estimations (Kane et al. 2016) place the inner edge of the habitable zone at  $1.5 F_\oplus$ , so planets b, c and d are closer to the star than the inner part of the habitable zone.

The amplitude of the signal in transit transmission spectroscopy can be estimated as  $\frac{R_p \cdot h_{\text{eff}}}{(R_*)^2}$  (Gillon et al. 2016) with  $h_{\text{eff}}$  the effective atmospheric height, which is related to the atmospheric scale height  $H = K \cdot T / \mu \cdot g$  ( $K$  Boltzmann's constant,  $T$  atmospheric temperature,  $\mu$  atmospheric mean molecular mass,  $g$  surface gravity). We adopt  $h_{\text{eff}} = 7 \cdot H$  (Miller-Ricci & Fortney 2010) for a transparent volatile dominated atmosphere ( $\mu = 20$ ) with 0.3 Bond albedo. With these assumptions we estimate the amplitudes of transit transmission spectroscopy signals as  $2.2 \cdot 10^{-5}$  (b),  $3.5 \cdot 10^{-5}$  (c) and  $1.2 \cdot 10^{-5}$  (d).

We tested the stability of the system simulating its evo-

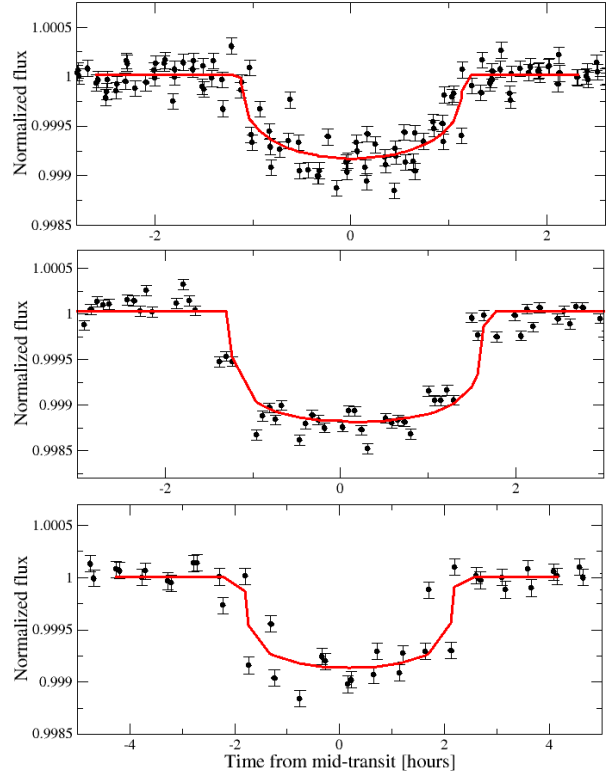


**Figure 4.** Phase-folded light curves corresponding to planets b (top), c (middle), and d (bottom). Solid curves represent best model fits obtained by MCMC.

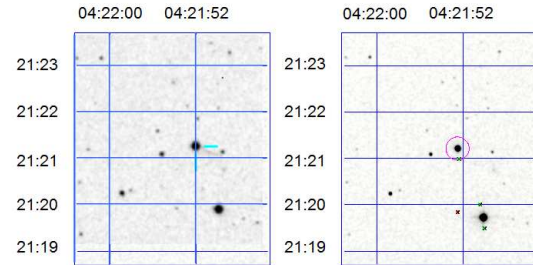


**Figure 5.** POSS-I image (1953, left) and 2MASS (1998, right). No background source is present at star's position in K2 13<sup>th</sup> campaign.

lution for  $10^6$  years with the Mercury package (Chambers 1999), using Bulirsch – Stoer integrator, adopting circular orbits and masses from the mass - radius relation. Our simulations show no significant changes in the eccentricity (always below 0.0005 for all the planets) or in the inclination of the orbits (always below  $1.6^\circ$ ,  $1.2^\circ$  and  $1^\circ$  for planets b, c and d), pointing toward a dynamically stable system.

## 4 CONCLUSIONS

We presented a system with three transiting super-Earths orbiting a mid-late type K-dwarf star, discovered with photometric data from K2. The star has been studied and characterized in detail, analyzing its spectrum and long time photometric series. The detected planets have radii  $1.8^{+0.2}_{-0.1}$



**Table 2.** Parameters for planets b, c and d.

Planet Parameters	b	c	d		
Orbital period (P) [d]	6.342±0.002	13.850±0.006	40.718±0.005		
Semi-major axis (a) [AU]	0.0562 <sup>+0.0013</sup> <sub>-0.0014</sub>	0.0946 <sup>+0.0031</sup> <sub>-0.0030</sub>	0.1937 <sup>+0.0064</sup> <sub>-0.0059</sub>		
Radius ( $R_p$ ) [ $R_\oplus$ ]	1.8 <sup>+0.2</sup> <sub>-0.1</sub>	2.6 <sup>+0.7</sup> <sub>-0.2</sub>	1.9 <sup>+0.7</sup> <sub>-0.2</sub>		
Mass ( $M_p$ ) [ $M_\oplus$ ] (1)	4.7 <sup>+0.5</sup> <sub>-0.3</sub>	6.5 <sup>+1.5</sup> <sub>-0.5</sub>	4.9 <sup>+1.7</sup> <sub>-0.6</sub>		
Equilibrium Temperature ( $T_{eq}$ ) [K]	708 <sup>+38</sup> <sub>-31</sub>	583 <sup>+52</sup> <sub>-35</sub>	381 <sup>+47</sup> <sub>-25</sub>		
Transit Parameters	b	c	d	d (2990.500) (2)	d (3031.218) (2)
Number of transits	12	5	2	–	–
Epoch (BKJD) [days]	2992.068±0.002	2995.426±0.001	2990.500±0.003	2990.500±0.003	3031.218±0.002
Radius of planet in stellar radii ( $R_p/R_*$ )	0.0261 <sup>+0.0009</sup> <sub>-0.0008</sub>	0.0321 <sup>+0.0016</sup> <sub>-0.0010</sub>	0.0273 <sup>+0.0021</sup> <sub>-0.0015</sub>	0.0280 <sup>+0.0011</sup> <sub>-0.0009</sub>	0.0292 <sup>+0.0027</sup> <sub>-0.0018</sub>
Semi major axis in stellar radii (a/ $R_*$ )	18.5 <sup>+0.1</sup> <sub>-1.6</sub>	27.0 <sup>+2.2</sup> <sub>-4.2</sub>	63.3 <sup>+6.4</sup> <sub>-13</sub>	73.2 <sup>+4.2</sup> <sub>-6.7</sub>	75.0 <sup>+13</sup> <sub>-20</sub>
Linear limb-darkening coeff ( $u_1$ )	0.644 <sup>+0.063</sup> <sub>-0.080</sub>	0.614 <sup>+0.065</sup> <sub>-0.084</sub>	0.597 <sup>+0.085</sup> <sub>-0.110</sub>	0.551 <sup>+0.083</sup> <sub>-0.11</sub>	0.540 <sup>+0.10</sup> <sub>-0.12</sub>
Quadratic limb-darkening coeff ( $u_2$ )	0.122 <sup>+0.074</sup> <sub>-0.061</sub>	0.148 <sup>+0.071</sup> <sub>-0.060</sub>	0.142 <sup>+0.091</sup> <sub>-0.072</sub>	0.174 <sup>+0.093</sup> <sub>-0.077</sub>	0.183 <sup>+0.11</sup> <sub>-0.088</sub>
Inclination (i) [deg]	88.3 <sup>+1.2</sup> <sub>-1.9</sub>	88.96 <sup>+0.71</sup> <sub>-0.88</sub>	89.61 <sup>+0.27</sup> <sub>-0.48</sub>	89.75 <sup>+0.17</sup> <sub>-0.20</sub>	89.62 <sup>+0.26</sup> <sub>-0.37</sub>
Impact Parameter (b)	0.34 <sup>+0.24</sup> <sub>-0.23</sub>	0.45 <sup>+0.37</sup> <sub>-0.31</sub>	0.44 <sup>+0.33</sup> <sub>-0.30</sub>	0.33 <sup>+0.20</sup> <sub>-0.21</sub>	0.50 <sup>+0.22</sup> <sub>-0.31</sub>
Transit depth ( $\delta$ )	0.00068 <sup>+0.00005</sup> <sub>-0.00004</sub>	0.00103 <sup>+0.00010</sup> <sub>-0.00006</sub>	0.00074 <sup>+0.00012</sup> <sub>-0.00008</sub>	0.00078 <sup>+0.00006</sup> <sub>-0.00005</sub>	0.00085 <sup>+0.00017</sup> <sub>-0.00010</sub>
Total duration ( $T_{14}$ ) [days]	0.1004 <sup>+0.0050</sup> <sub>-0.0048</sub>	0.1470 <sup>+0.0130</sup> <sub>-0.0260</sub>	0.1860 <sup>+0.0097</sup> <sub>-0.0018</sub>	0.1713 <sup>+0.0056</sup> <sub>-0.0051</sub>	0.156 <sup>+0.018</sup> <sub>-0.011</sub>
Ingress/egress duration ( $\tau$ ) [days]	0.0030 <sup>+0.0009</sup> <sub>-0.0003</sub>	0.0056 <sup>+0.0039</sup> <sub>-0.0008</sub>	0.0060 <sup>+0.0050</sup> <sub>-0.0010</sub>	0.0052 <sup>+0.0014</sup> <sub>-0.0005</sub>	0.0058 <sup>+0.0049</sup> <sub>-0.0016</sub>

(1): The masses are estimated using mass-radius relation from Weiss &amp; Marcy (2014).

(2): Derived parameters for individual transits of planet d.

$R_\oplus$ (b),  $2.6^{+0.7}_{-0.2} R_\oplus$ (c),  $1.9^{+0.7}_{-0.2} R_\oplus$  (c) and orbital periods 6.342±0.002 days (b), 13.850±0.006 days (c), 40.718±0.005 days (d). Additional photometric monitoring is required to confirm planet d and radial velocity monitoring with ultra-stable spectrographs at 8-10 m telescopes is necessary to determine accurate planetary masses. The amplitudes of atmospheric signals in transmission spectroscopy have been estimated at ~ 20 ppm, making the system a good target to incoming facilities such as James Webb Telescope.

## REFERENCES

- Allende Prieto, C., Fernández-Alvar, E., Schlesinger, K. J., et al. 2014, *A&A*, 568, A7
- Bensby, T., Oey, M. S., Feltzing, S., Gustafsson, B. 2007, *ApJ*, 655, L89
- Bertelli, G., Bressan, A., Chiosi, C., Fagotto, F., Nasi, E. 1994, *A&AS*, 106, 275
- Bonifacio, P., Monai, S., Beers, T. C. 2000, *AJ*, 120, 2065
- Borucki, W. J., Koch, D., Basri, G., et al. 2010, *Science*, 327, 977
- Castelli, F., Kurucz, R. L. 2003, *Modelling of Stellar Atmospheres*, 210, A20
- Cauley, P. W., Redfield, S., Jensen, A. G. 2017, *AJ*, 153, 185
- Chambers, J. E. 1999, *MNRAS*, 304, 793
- Charbonneau, D., Brown, T. M., Latham, D. W., Mayor, M. 2000, *ApJ*, 529, L45
- Cosentino, R., Lovis, C., Pepe, F., et al. 2012, *Proc. SPIE*, 8446, 84461V
- Crossfield, I. J. M., Ciardi, D. R., Petigura, E. A., et al. 2016, *ApJS*, 226, 7
- Cutri, R. M., Skrutskie, M. F., van Dyk, S., et al. 2003, *Eastman, J., Gaudi, B. S., Agol, E.* 2013, *PASP*, 125, 83
- Fischer, D. A., Valenti, J. 2005, *ApJ*, 622, 1102
- Gillon, M., Jehin, E., Lederer, S. M., et al. 2016, *Nature*, 533, 221
- González Hernández, J. I., Bonifacio, P. 2009, *A&A*, 497, 497
- González Hernández, J. I., Pepe, F., Molaro, P., & Santos, N. 2017, arXiv:1711.05250
- Gray, D. F. 2005, *The Observation and Analysis of Stellar Photospheres*. Cambridge University Press, Cambridge, England.
- Howard, A. W., Marcy, G. W., Bryson, S. T., et al. 2012, *ApJS*, 201, 15
- Howell, S. B., Sobeck, C., Haas, M., et al. 2014, *PASP*, 126, 398
- Kane, S. R., Hill, M. L., Kasting, J. F., et al. 2016, *ApJ*, 830, 1
- Koesterke, L., Allende Prieto, C., Lambert, D. L. 2008, *ApJ*, 680, 764-773
- Kordopatis, G., Gilmore, G., Steinmetz, M., et al. 2013, *AJ*, 146, 134
- Kovács, G., Zucker, S., Mazeh, T. 2002, *A&A*, 391, 369
- Kreidberg, L., Bean, J. L., Désert, J.-M., et al. 2014, *Nature*, 505, 69
- Lissauer, J. J., Ragozzine, D., Fabrycky, D. C., et al. 2011, *ApJS*, 197, 8
- McCall, M. L. 2004, *AJ*, 128, 2144
- Mészáros, S., Allende Prieto, C., Edvardsson, B., et al. 2012, *AJ*, 144, 120
- Miller-Ricci, E., Fortney, J. J. 2010, *ApJ*, 716, L74
- Minkowski, R. L., Abell, G. O. 1963, *Basic Astronomical Data: Stars and Stellar Systems*, 481
- Nordström, B., Mayor, M., Andersen, J., et al. 2004, *A&A*, 418, 989
- Owen, T., Mahaffy, P., Niemann, H. B., et al. 1999, *Nature*, 402, 269
- Pepe, F., Molaro, P., Cristiani, S., et al. 2014, *Astronomische Nachrichten*, 335, 8
- Pollacco, D. L., Skillen, I., Collier Cameron, A., et al. 2006, *PASP*, 118, 1407
- Rogers, L. A. 2015, *ApJ*, 801, 41
- Scargle, J. D. 1982, *ApJ*, 263, 835
- Schlegel, D. J., Finkbeiner, D. P., Davis, M. 1998, *ApJ*, 500, 525
- Suárez Mascareño, A., Rebolo, R., González Hernández, J. I., Esposito, M. 2015, *MNRAS*, 452, 2745
- Suárez Mascareño, A., Rebolo, R., González Hernández, J. I.

- 2016, A&A, 595, A12  
Suárez Mascareño, A., Rebolo, R., González Hernández, J. I.,  
Esposito, M. 2017, MNRAS, 468, 4772  
Van Eylen, V., Albrecht, S. 2015, ApJ, 808, 126  
Vanderburg, A., Johnson, J. A. 2014, PASP, 126, 948  
Vanderburg, A., Montet, B. T., Johnson, J. A., et al. 2015, ApJ,  
800, 59  
Weiss, L. M., Marcy, G. W. 2014, ApJ, 783, L6  
Zacharias, N., Finch, C. T., Girard, T. M., et al. 2013, AJ, 145,  
44

This paper has been typeset from a  $\text{\TeX}/\text{\LaTeX}$  file prepared by  
the author.